Microelectronic Engineering 88 (2011) 1240–1242

Contents lists available at ScienceDirect

Microelectronic Engineering

journal homepage: www.elsevier.com/locate/mee

Nanosized metal grains induced electrical characteristic fluctuation in 16-nm-gate high-κ/metal gate bulk FinFET devices

Yiming Li [a,b,*], Hui-Wen Cheng [b], Chun-Yen Yiu [b], Hsin-Wen Su [a]

[a] Department of Electrical Engineering, National Chiao Tung University, Hsinchu 300, Taiwan
[b] Institute of Communications Engineering, National Chiao Tung University, Hsinchu 300, Taiwan

ARTICLE INFO

Article history:
Available online 30 March 2011

Keywords:
Metal gate
TiN gate
Random work function
Bulk FinFET
Threshold voltage fluctuation
Random grain's size
Number and position
Large scale 3D device simulation

ABSTRACT

In this work, the work function fluctuation (WKF) induced variability in 16-nm-gate bulk N-FinFET is for the first time explored by an experimentally calibrated 3D device simulation. Random nanosized grains of TiN gate are statistically positioned in the gate region to examine the associated carriers' transport, concurrently capturing "grain number variation" and "grain position fluctuation." The newly developed localized WKF simulation method enables us to estimate the threshold voltage fluctuation of devices with respect to the aspect ratio (AR = fin height/fin width) which accounts for the random grain's size, number and position effects simultaneously.

1. Introduction

Devices with vertical channel possess diverse fascinating characteristics [1]. High-κ/metal gate stacked fin-type field-effect-transistor (FinFET) is promising technology in sub-22 nm device era [2–4]. However, metal gate may introduce random fluctuation source, so-called the work function fluctuation (WKF) owing to the dependency of work function on metal grain's size, number and position. Such uncontrollable grain orientations result in random work function of metal during growth period [2–7]. Many studies concerning WKF on planar CMOS technology have been reported [3–7]. Unfortunately, effect of localized WKF [2] on electrical characteristics with respect to the aspect ratio of bulk FinFET have not been explored yet. In this study, based on the experimentally calibrated 3D device simulation [8], WKF of bulk N-FinFET with TiN/HfO_2 gate stack and AR = 1 and 2 are investigated. Notably, the influence of random grain's size, number and position effects is thus discussed.

2. Simulation methodology

The devices we examined are the 16-nm-gate bulk N-FinFETs with amorphous-based TiN/HfO_2 gate stack and an EOT of 0.8 nm, where the devices are with two different aspect ratios, AR = 1 and 2. Fig. 1(a) shows the validated performance of bulk N-FinFETs according to ITRS roadmap for low operating power [9]. Different from the average WKF (AWKF) method [3,4] and the compact model approach [10], we present the localized WKF (LWKF) method [2] which directly partitions the area of device's metal gate into 48 and 80 sub-regions following Gaussian distribution, where the average number of total generated ⟨2 0 0⟩ orientations are 28 and 48 for AR = 1 and 2, as shown in Fig. 1(b), respectively. Then, we randomly generate the work function to each sub-region according to material's property listed in Fig. 1(c), where ⟨2 0 0⟩ and ⟨1 1 1⟩ grain orientations of TiN gate have relatively close probabilities 60% and 40%. Then, the 196 cases are generated and mapped into device gate area for 3D device simulation [8].

3. Results and discussion

The AWKF and LWKF methods induce rather different potential profile of the channel surface, as shown in Fig. 2(a). The potential profile induced by the AWKF method is smooth while the potential profile is strongly governed by the different work function locally. The comparison of $\sigma_{V_{th}}$ between AWKF and LWKF methods for the devices with different aspect ratio is shown in Fig. 2(b). The fluctuation induced by the AWKF method may underestimate because it does not consider the effect of localized work function individually. Fig. 2(c) presents the I_D–V_G curves in which the red and blue lines

* Corresponding author. at: Department of Electrical Engineering, National Chiao Tung University, Hsinchu 300, Taiwan. Tel.: +886 3 5712121x52974; fax: +886 3 5726639.

0167-9317/$ - see front matter © 2011 Elsevier B.V. All rights reserved.
doi:10.1016/j.mee.2011.03.037

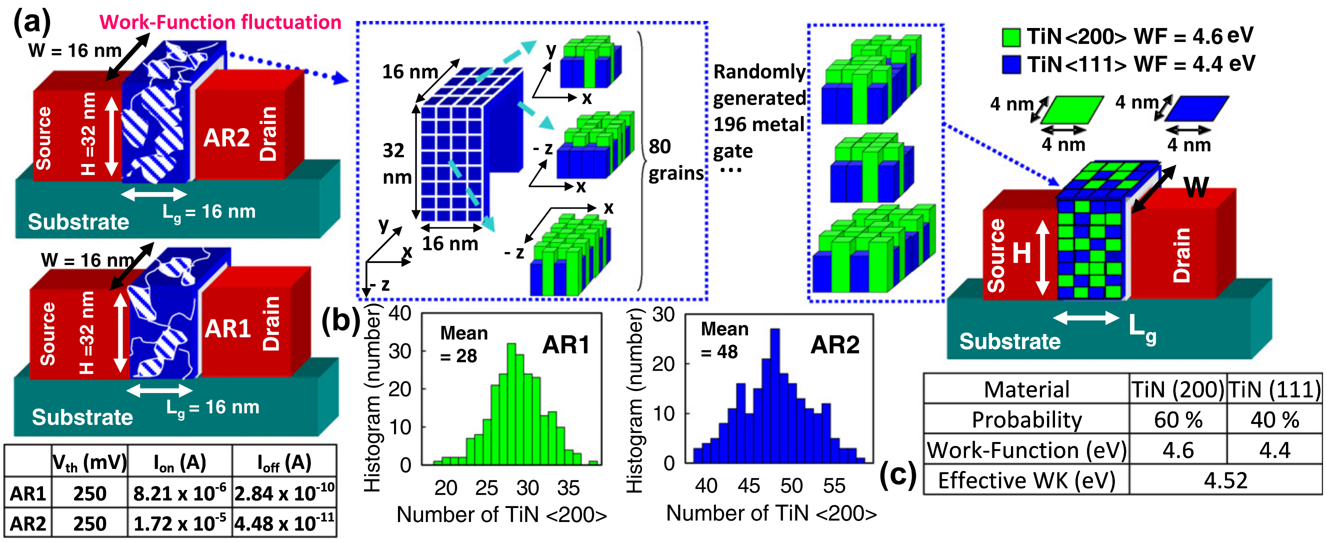

Fig. 1. (a) Schematic of the simulated bulk N-FinFET with random metal grain on the gate and the achieved device performance for AR = 1 and AR = 2. (b) 48 and 80 randomly generated grains in each device with AR = 1 and with AR = 2, where the size of metal grain are $4 \times 4\ \text{nm}^2$ and green and blue colors are ⟨2 0 0⟩ and ⟨1 1 1⟩ orientations, respectively. The mean numbers of TiN ⟨2 0 0⟩ orientations are 28 and 48 for generated 196 devices with AR = 1 and 2, respectively. (c) The material property of TiN.

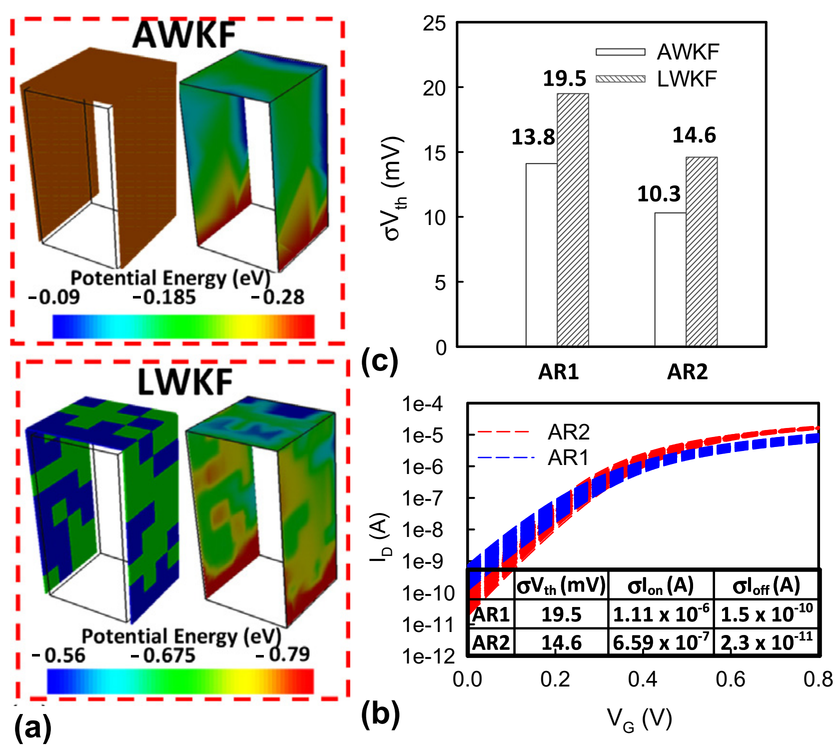

Fig. 2. (a) The potential profiles calculated by AWKF and LWKF methods. (b) Comparison of $\sigma_{V_{th}}$ between the AWKF and LWKF methods for devices with AR = 1 and 2. The A_{vt} of AR = 1 and 2 for AWKF are 0.88 and 1.22, respectively; for LWKF method, they are 0.64 and 0.91, where the A_{vt} is calculated by $\sigma_{V_{th}} \times (LW)^{0.5}$. (c) The I_D–V_G plot of the studied devices with AR = 1 and 2, where the values of $\sigma_{V_{th}}$, $\sigma_{I_{on}}$ and $\sigma_{I_{off}}$ are summarized.

are the devices with AR = 1 and 2, respectively, where $\sigma_{V_{th}}$, $\sigma_{I_{on}}$ and $\sigma_{I_{off}}$ are summarized in inset. The device with AR = 2 shows better control channel controllability, where the $\sigma_{V_{th}}$ of AR = 2 is 1.3 times smaller than that of AR = 1. Fig. 3(a) shows the plot of on-state current (I_{on}) versus off-state current (I_{off}) for the device with different aspect ratio. It indicates the device with AR = 2 shows smaller deviation owing to better channel controllability. I_{on} and I_{off} characteristics depending on random grain number and position effects are further studied. We examine the cross-sectional (top-view) on-state ($V_D = V_G = 0.8$ V) current density and off-state ($V_D = 0.8$ V, $V_G = 0$V) electrostatic potential of channel surface. Fig. 3(b″–d″) show the top-view of on-state current density and the Figs 3(b′–d′) show the top-view of off-state potential profile. Compared the current density, as shown in Fig. 3(b″ and c″), the similar I_{on} with different I_{off} mechanisms induced different current density due to random grain position effect. In contrast, the similar I_{off} with different I_{on} mechanisms due to random grain number effect can be explained by top view of potential profile as shown in Fig. 3(b′ and d′). Further, we also consider the grain size's effect for the device with different aspect ratio, where the grain size are (2 × 2),

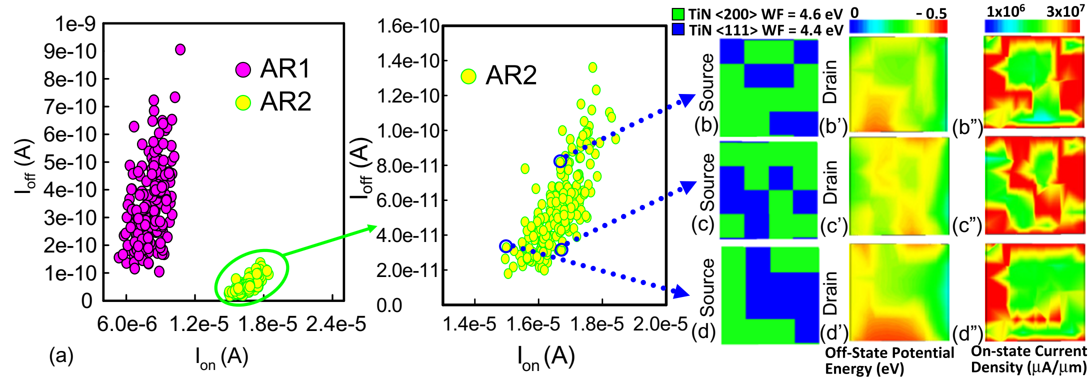

Fig. 3. (a) The characteristics of I_{off} versus I_{on} for the bulk N-FinFET with AR = 1 and 2. Three different cases are selected to evaluate similar I_{off} but different I_{on} (plots of (b and c)) and similar I_{on} but different I_{off} (plots of (c and d)). Plots of (b″ and c″) show the corresponding top-views of on-state current density, similar I_{on} with different I_{off} mechanisms induced different current density due to random grain position effect. Plots of (c′ and d′) show the corresponding top-views of off-state potential profile, the similar I_{off} with different I_{on} mechanisms due to random grain number effect can be explained.

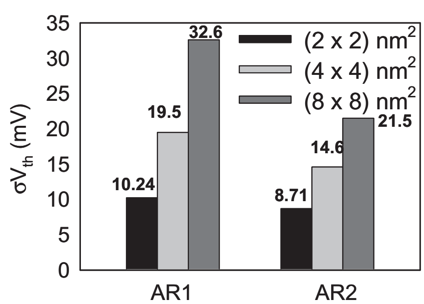

Fig. 4. The $\sigma_{V_{th}}$ induced by different grain sizes: (2 × 2), (4 × 4) and (8 × 8) nm^2 for the bulk N-FinFET with AR = 1 and AR = 2, respectively. The A_{vt} of (2 × 2), (4 × 4) and (8 × 8) nm^2 for N-FinFET with AR = 1 are 0.64, 1.22 and 2.03, respectively; for N-FinFET with AR = 2, they are 0.54, 0.91 and 1.34.

(4 × 4) and (8 × 8) nm^2, respectively, as shown in Fig. 4. The $\sigma_{V_{th}}$ induced by the grain size of (2 × 2) nm^2 is 10.24 and 8.71 mV for the device with AR = 1 and 2, which is 3.2 and 2.6 times smaller than the grain size of (8 × 8) nm^2 for the device with AR = 1 and 2, respectively.

4. Conclusions

In this study, the LWKF simulation method was advanced to study the WKF-induced variability in 16-nm-gate bulk N-FinFETs with amorphous-based TiN/HfO_2 gate stacks. Based on this method, for device with AR = 1, $\sigma_{V_{th}}$ = 19.5 mV and for AR = 2, $\sigma_{V_{th}}$ = 14.6 mV; consequently, the fluctuations resulting from random grains' number and position were estimated and the WKF is suppressed by device with higher AR. Further, we examined the grain size's effect. As the grain size increases from (2 × 2) to (8 × 8) nm^2, the $\sigma_{V_{th}}$ increases from 10.24 and 8.71 mV to 32.6 and 21.5 mV for the FinFET with AR = 1 and 2. However, for more completed consideration, process variation effect (PVE) should also be addressed for N-FinFET devices. We are currently studying the WKF and PVE using a unified computational model with comparing with fabricated bulk FinFET devices.

Acknowledgements

This work was supported in part by National Science Council (NSC), Taiwan under Contract No. NSC-99-2221-E-009-175 and by TSMC, Hsinchu, Taiwan under a 2010-2011 grant.

References

[1] Y. Li, C.-H. Hwang, IEEE Trans. Electron Devices 54 (2007) 3426–3429.
[2] H.-W. Cheng, F.-H. Li, M.-H. Han, C.-Y. Yiu, C.-H. Yu, K.-F. Lee, Y. Li, IEDM Tech. Dig. (2010) 379–382.
[3] H.F. Dadgour, K. Endo, V. De, K. Banerjee, IEDM Tech. Dig. (2008) 705–708.
[4] H.F. Dadgour, K. Endo, V.K. De, K. Banerjee, IEEE Trans. Electron Devices 57 (2010) 2504–2514.
[5] A.R. Brown, N.M. Idris, J.R. Watling, A. Asenov, IEEE Electron Device Lett. 31 (11) (2010) 1199–1201.
[6] A. Yagishita, T. Saito, K. Nakajima, S. Inumiya, K. Matsuo, T. Shibata, Y. Tsunashima, K. Suguro, T. Arikado, IEEE Trans. Electron Devices 48 (2001) 1604–1611.
[7] X. Zhang, J. Li, M. Grubbs, M. Deal, B. Magyari-Kope, B.M. Clemens, Y. Nishi, IEDM Tech. Dig. (2009) 57–60.
[8] Y. Li, S.-M. Yu, J.-R. Hwang, F.-L. Yang, IEEE Trans. Electron Devices 55 (2008) 1449–1455.
[9] <http://www.itrs.net>.
[10] X. Chen, S. Samavedam, V. Narayanan, K. Stein, C. Hobbs, C. Baiocco, W. Li, D. Jaeger, M. Zaleski, H.-S. Yang, N. Kim, Y. Lee, D. Zhang, L. Kang, J. Chen, H. Zhuang, A. Sheikh, J. Wallner, M. Aquilino, J. Han, Z. Jin, J. Li, G. Massey, S. Kalpat, R. Jha, N. Moumen, R. Mo, S. Kirshnan, X. Wang, M. Chudzik, M. Cjowdhury, D. Nair, C. Reddy, Y. -W. Teh, C. Kothandaraman, D. Coolbaugh, S. Pandey, D. Tekleab, A. Thean, M. Sherony, C. Lage, J. Sudijono, R. Lindsay, J.-H. Ku, M. Khare, and A. Steegen, VLSI Symp. Tech. Dig., 2008, pp. 88–89.